

# Chapter 3

## The Pathology of Common Sinonasal and Skull Base Malignancies



Ying-Hsia Chu, Peter M. Sadow, and William C. Faquin

### Introduction

Within a relatively small anatomic space, the sinonasal tract gives rise to a tremendous variety of neoplasms. In the current (2017) version of the World Health Organization classification (Table 3.1) [1], the primary malignant neoplasms of the nasal cavity, paranasal sinuses, and skull base are divided into six major categories based on the presumed cell type of origin or the direction of differentiation: (1) sinonasal carcinomas (epithelial-derived tumors), (2) salivary-type neoplasia, (3) neuroectodermal/melanocytic tumors, (4) mesenchymal neoplasms, (5) hematolymphoid malignancies, and (6) teratocarcinomas. Sinonasal malignancies are overall uncommon, accounting for less than 1% of all cancers at this site and less than 3% of upper aerodigestive tract cancers in the United States. The most common histologic types are squamous cell carcinoma (SCC; 40% of all sinonasal cancers), adenocarcinoma (13%), melanoma (12%), lymphoma (11%), adenoid cystic carcinoma (7%), undifferentiated carcinoma (7%), and olfactory neuroblastoma (ONB; 4%) [2].

Biopsy to obtain a histologic diagnosis is the first step in the management of sinonasal cancers, as the therapeutic approach varies significantly by tumor type. In the current National Comprehensive Cancer Network (NCCN) guidelines ([www.nccn.org](http://www.nccn.org)), sinonasal carcinomas (including squamous cell carcinomas, adenocarcinomas, neuroendocrine carcinomas), olfactory neuroblastomas, and salivary-type

---

Y.-H. Chu  
Pathology, Chang Gung Memorial Hospital, Taoyuan City, Taiwan

P. M. Sadow · W. C. Faquin (✉)  
Department of Pathology, Massachusetts General Hospital and Harvard Medical School,  
Boston, MA, USA  
e-mail: [psadow@mgh.harvard.edu](mailto:psadow@mgh.harvard.edu); [wfaquin@mgh.harvard.edu](mailto:wfaquin@mgh.harvard.edu)

**Table 3.1** World Health Organization classification of sinonasal and skull base malignancies

<b>Carcinomas</b>	<b>Malignant soft tissue tumors</b>
Keratinizing squamous cell carcinoma	Fibrosarcoma
Non-keratinizing squamous cell carcinoma	Undifferentiated pleomorphic sarcoma
Spindle cell squamous cell carcinoma	Leiomyosarcoma
Lymphoepithelial carcinoma	Rhabdomyosarcoma, not otherwise specified
Sinonasal undifferentiated carcinoma	Embryonal rhabdomyosarcoma
NUT carcinoma	Alveolar rhabdomyosarcoma
Neuroendocrine carcinomas	Pleomorphic rhabdomyosarcoma, adult type
Small cell neuroendocrine carcinoma	Spindle cell rhabdomyosarcoma
Large cell neuroendocrine carcinoma	Angiosarcoma
Adenocarcinomas	Malignant peripheral nerve sheath tumor
Intestinal-type adenocarcinoma	Biphenotypic sinonasal sarcoma
Non-intestinal-type adenocarcinoma	Synovial sarcoma
<b>Salivary gland tumors</b>	<b>Borderline/low-grade malignant soft tissue tumors</b>
	Desmoid-type fibromatosis
<b>Neuroectodermal/melanocytic tumors</b>	Sinonasal glomangiopericytoma
Mucosal melanoma	Solitary fibrous tumor
Olfactory neuroblastoma	Epithelioid hemangioendothelioma
Ewing sarcoma/primitive neuroectodermal tumor	
<b>Hematolymphoid tumors</b>	<b>Teratocarcinosarcoma</b>
Extranodal NK-/T-cell lymphoma	
Extraosseous plasmacytoma	

neoplasias are treated with similar approaches that include primary resection and contingent adjuvant chemoradiation. Pathologists play an essential role in identifying key microscopic features that would trigger adjuvant therapy, including high histologic grade, positive margins, perineural and/or lymphovascular invasion, extranodal extension, and certain histologic types such as sinonasal undifferentiated carcinoma (SNUC) with neuroendocrine features, neuroendocrine carcinoma (NEC), and high-grade olfactory neuroendocrine carcinoma.

Despite aggressive clinical intervention, the overall outlook for patients with sinonasal cancers remains grim, with collective 5-, 10-, and 20-year survival being 45.7%, 32.2%, and 16.4%, respectively, in a recent study [3]. This reflects the fact that up to 51% of patients present at a high stage (III–IV), 50% have locally advanced (T3–T4) tumors, 6% have lymph node involvement (N1–N2), and 6% show distant metastatic disease at the time of initial diagnosis [4]. As ongoing research continues to uncover actionable genetic abnormalities in sinonasal malignancies, the development of novel targeted therapies represents a promising lead for patient outcome improvement. Some examples include the imatinib treatment in mucosal melanoma and the recent discovery of recurrent *IDH2* mutations in SNUC, as discussed later in this chapter.

## Squamous Cell Carcinomas

### *Definition and Clinical Background*

Squamous cell carcinomas are a group of malignant epithelial neoplasms with squamous differentiation. Being the most common histologic type of sinonasal cancers, squamous cell carcinomas account for 40% of the cases, and most cases present in the sixth and seventh decades of life with a male-to-female ratio of approximately 2:1. Reported risk factors include cigarette smoking and industrial exposures such as wood and leather dust [5]. Tumors arising in the nasal cavity and the paranasal sinuses each account for about half of the cases. Lymph node involvement is present in 10–20% of patients at initial presentation [6].

### *Pathology*

Sinonasal squamous cell carcinoma may present with various histologic subtypes, primarily keratinizing (50% of cases) and non-keratinizing (33%), but also with variants such as basaloid (7%), papillary (5%), adenosquamous (5%), and spindle cell (2%) [6]. Keratinizing squamous cell carcinomas have irregular nests of tumor cells with keratin-rich, brightly eosinophilic cytoplasm and the presence of intercellular bridges (Fig. 3.1a). The non-keratinizing subtype is

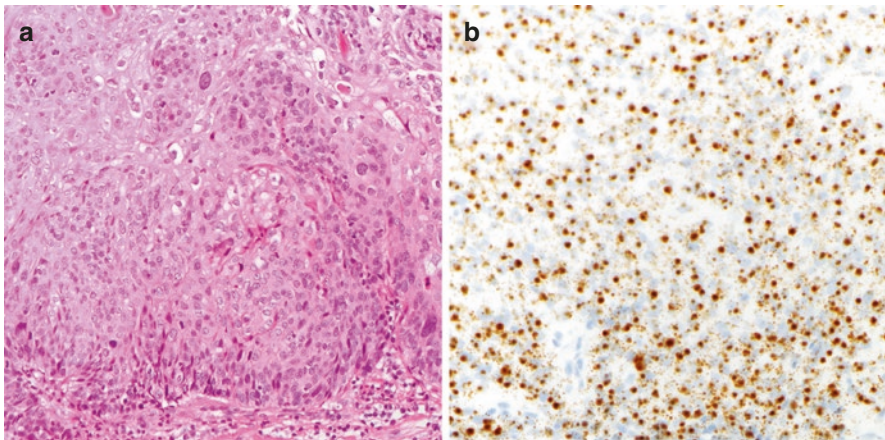


**Fig. 3.1** Squamous cell carcinoma, keratinizing. **(a)** Nested growth of tumor cells with moderate anisonucleosis and abundant eosinophilic cytoplasm. **(b)** Only approximately 4% of cases are associated with high-risk human papillomavirus, as demonstrated here by chromogenic in situ hybridization for HPV types 16 and 18

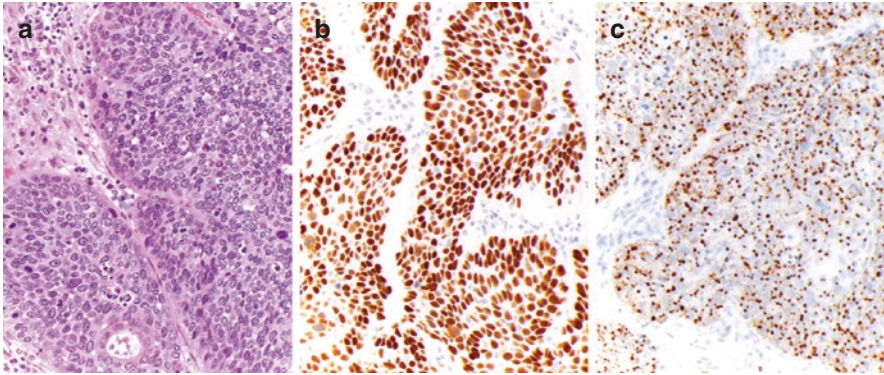


**Fig. 3.2** Squamous cell carcinoma, non-keratinizing, showing a lobulated growth pattern of immature squamous cells with a smooth pushing interface within the stroma and with abundant mitoses (a). There is diffuse nuclear p40 expression (b). In around 41% of cases, high-risk human papillomavirus can be detected by PCR or chromogenic in situ hybridization (c, with probes for HPV types 16 and 18)

characterized by a nested to ribbon-like growth pattern and a basophilic, immature cytologic appearance with elevated nuclear-to-cytoplasmic ratio and abundant mitotic activity (Fig. 3.2a). Squamous cell carcinomas of all subtypes exhibit diffuse expression of pancytokeratin (AE1/AE3), and high-molecular-weight keratins such as keratin 5/6, p40 (Fig. 3.2b), and p63. The rate of high-risk human papillomavirus (HPV) detection varies with histologic patterns, most frequent in the papillary subtype (80%), followed by the adenosquamous (67%), basaloid (46%), non-keratinizing (41%; Fig. 3.2c), and keratinizing (4%; Fig. 3.1b) cases [6]. The clinical significance of HPV in these cancers, however, is uncertain.

### ***Treatment and Prognosis***

Sinonasal squamous cell carcinomas are treated with surgical resection and adjuvant radiation. The overall clinical outlook is poor, with a 5- and 10-year overall survival of 30% and 21%, respectively [7]. Although the overall prognosis is poor, patients over the age of 50, particularly Black patients and/or those who present with advanced disease stage, have particularly unfavorable outcomes [7]. Additionally, some subtypes, such as basaloid squamous cell and adenosquamous carcinomas, tend to be more aggressive. As for the high-risk HPV status, some studies have suggested better survival in HPV-positive cases [8, 9]; however, the association is much less conclusive than in the oropharyngeal squamous cell carcinomas.

## **Non-salivary Sinonasal Adenocarcinoma**

### ***Definition and Clinical Background***

Sinonasal adenocarcinomas encompass a heterogeneous group of neoplasms with glandular differentiation arising from two possible origins: the submucosal seromucinous glands and the surface respiratory epithelium. The former give rise to various salivary gland tumors, the most frequent being adenoid cystic carcinoma, which is discussed in the next section of this chapter. Tumors arising from the respiratory epithelium constitute the category of non-salivary sinonasal adenocarcinoma, which is further divided into the intestinal and the non-intestinal types. Among a total of 325 cases of sinonasal adenocarcinomas in the Surveillance, Epidemiology, and End Results (SEER) database between 1988 and 2010, 300 (92.3%) were of the non-intestinal type and 25 (7.7%) were of the intestinal type [10]. Both types primarily occur in the sixth and seventh decades of life. Interestingly, around 80% of non-salivary sinonasal adenocarcinomas occur in Caucasians and 13% in African Americans, with only rare occurrence in other ethnicities. At the time of diagnosis, only 30.8% of patients had localized disease, while most patients already had regional or distant spread of tumor [10].

A strong association has been identified between the intestinal-type sinonasal adenocarcinoma and chronic exposure to wood dust [11]. Leather and textile dust as well as formaldehyde exposures have also been implicated. In a recent series of 117 cases of wood-dust-related, intestinal-type sinonasal adenocarcinoma, the duration of exposure ranged from 5 to 62 years, while the latency period ranged from 15 to 73 years [11]. Over 95% of the wood-dust-related cases are in males. In contrast, the non-intestinal-type sinonasal adenocarcinoma has no known risk factor and no gender predilection.

### ***Pathology***

The intestinal-type sinonasal adenocarcinoma resembles adenocarcinoma of the gastrointestinal tract, consisting of hyperchromatic, columnar neoplastic cells with variable degrees of mucin production and frequent necrosis, the so-called intestinal-type “dirty necrosis” (Fig. 3.3a). The neoplastic glands may be arranged in five major patterns proposed by Barnes [12]: papillary, colonic, solid, mucinous, and mixed. The papillary pattern resembles the villous colonic adenoma (Fig. 3.3a), while the mucinous pattern closely simulates mucinous (colloid) colorectal adenocarcinoma with copious mucin pools that contain dispersed tumor cells. By immunohistochemistry, the neoplastic cells are positive for CK20, CDX2 (Fig. 3.3b), SATB-2, villin, and MUC2. CK7 expression is variable. Clinical information, including colonoscopy findings, are essential for excluding the possibility of

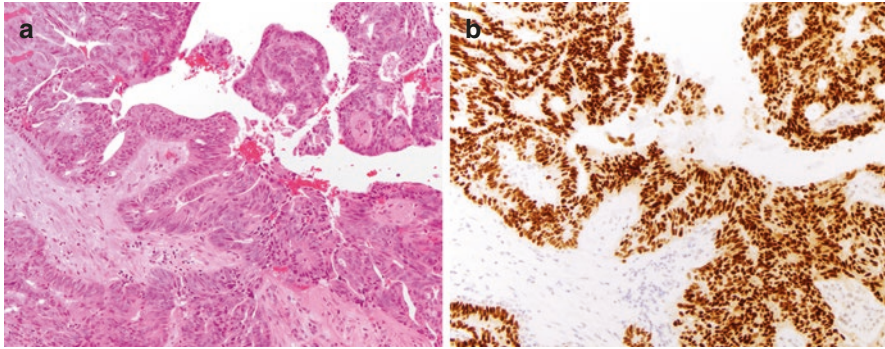


**Fig. 3.3** Intestinal-type sinonasal adenocarcinoma with papillary growth of columnar tumor cells with elongated, pseudostratified nuclei, resembling colorectal adenocarcinoma (a). There is diffuse nuclear expression of CDX2 (b)

metastatic adenocarcinoma from a gastrointestinal primary given the overlapping histomorphology and immunoprofile. Of note, CDX2 is not entirely specific in the sinonasal region for the intestinal-type sinonasal adenocarcinoma. Subsets of sinonasal undifferentiated carcinomas (38%), squamous cell carcinomas (10%), salivary gland tumors (10%), and small cell carcinomas (50%) may also express CDX2 but not CK20 [13]. Despite its morphologic resemblance to colorectal adenocarcinoma, *BRAF*, *KRAS*, and *EGFR* alterations and microsatellite instability are rare in the intestinal-type sinonasal adenocarcinoma. Instead, *TP53* mutations are commonly found in up to 86% of patients [14].

The non-intestinal-type sinonasal adenocarcinoma is a diagnostic term that encompasses all non-salivary sinonasal adenocarcinomas that lack the expression of intestinal markers (CK20, CDX2, SATB-2, villin, and MUC2). The morphological spectrum is broad, including high- and low-grade tumors with oncocytic, mucinous, or clear cell features (Fig. 3.4). There is diffuse cytoplasmic expression of CK7 and occasionally apical luminal staining for DOG1 (Fig. 3.4d). The molecular underpinning is highly heterogeneous and poorly understood. Recently, *ETV6* rearrangements, including *ETV6-NTRK3*, have been reported in a small series [15].

### ***Treatment and Prognosis***

Non-salivary sinonasal adenocarcinomas are treated with surgery and radiotherapy (RT). In the 1988–2010 SEER study, the 5-year disease-specific survival was 71.2% for the non-intestinal type and 69.3% for the intestinal type, with no statistically significant difference [10]. A single institutional series from Italy that included 30 intestinal-type cases reported a 5-year overall survival, disease-specific survival, disease-free survival, and recurrence-free survival of 72.7%, 78%, 67.9%, and 69.2%, respectively [16], similar to the SEER data. The same Italian institution subsequently published a separate series of 22 non-intestinal-type patients, in which

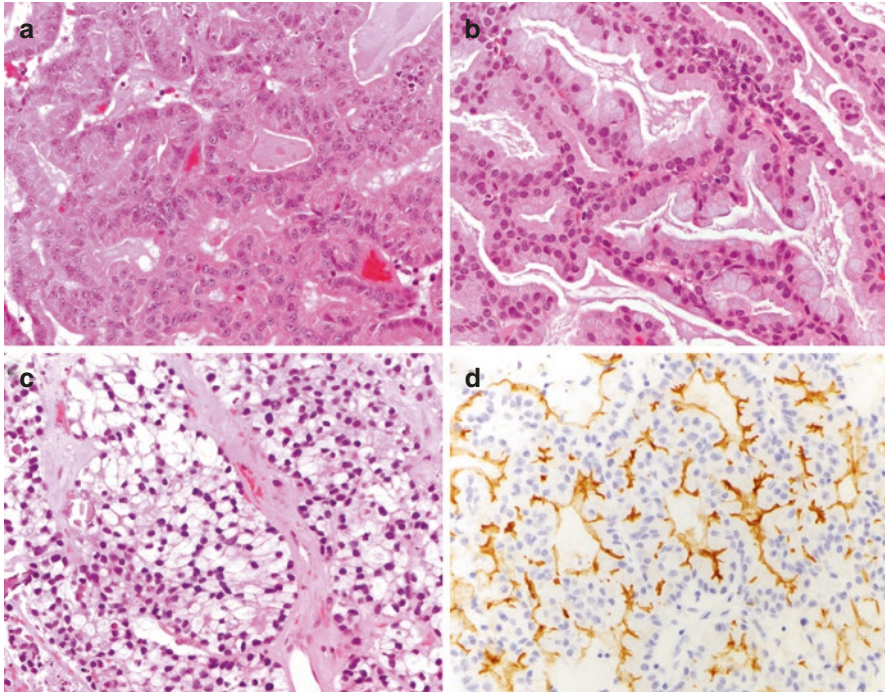


**Fig. 3.4** Non-intestinal-type sinonasal adenocarcinoma with various histologic appearances, such as granular and oncocyctic (a), mucin-producing (b), and clear cell (c). Occasionally, there might be luminal immunoreactivity to DOG1 (d), similar to the staining pattern seen in the acinic cell carcinoma of the salivary gland

a 5-year overall survival, disease-specific survival, and recurrence-free survival of 95.2%, 95.2%, and 90.4%, respectively, were reported [17]. Shorter survival has been associated with Black race, age at or above 75 years, paranasal sinus involvement, surgical resection, high histologic grade, positive surgical margin, and locally advanced or recurrent disease [10, 16, 17].

## Adenoid Cystic Carcinoma

### *Definition and Clinical Background*

Primary minor salivary gland carcinomas account for around 10% of sinonasal cancers, with adenoid cystic carcinomas being the most common histologic type (constituting 63% of cases), followed by mucoepidermoid carcinoma (8%) and polymorphous adenocarcinoma (5%) [18]. Based on a recent analysis of the SEER database between 2004 and 2012, the average presenting age for sinonasal adenoid cystic carcinoma was 59.6 years with roughly equal gender distribution [19]. Most

patients present with locally advanced disease (49% T4, 23% T3, 26% T2, 3% T1 [20]), with the maxillary sinus being the most frequent primary site. Lymph node involvement and distant metastases were seen in 3.6% and 3.7% of patients, respectively, at the time of diagnosis [19].

## Pathology

Adenoid cystic carcinoma consists of neoplastic cells with admixed ductal and myoepithelial differentiation forming cribriform, tubular, and solid growth patterns in variable proportions. The cribriform pattern is characterized by nests of basaloid cells that contain multiple punched-out spaces in a “Swiss cheese” appearance (Fig. 3.5). The spaces are lined by ductal-type cells with eosinophilic cytoplasm and well-delineated luminal borders, and are filled with basophilic hyaline material

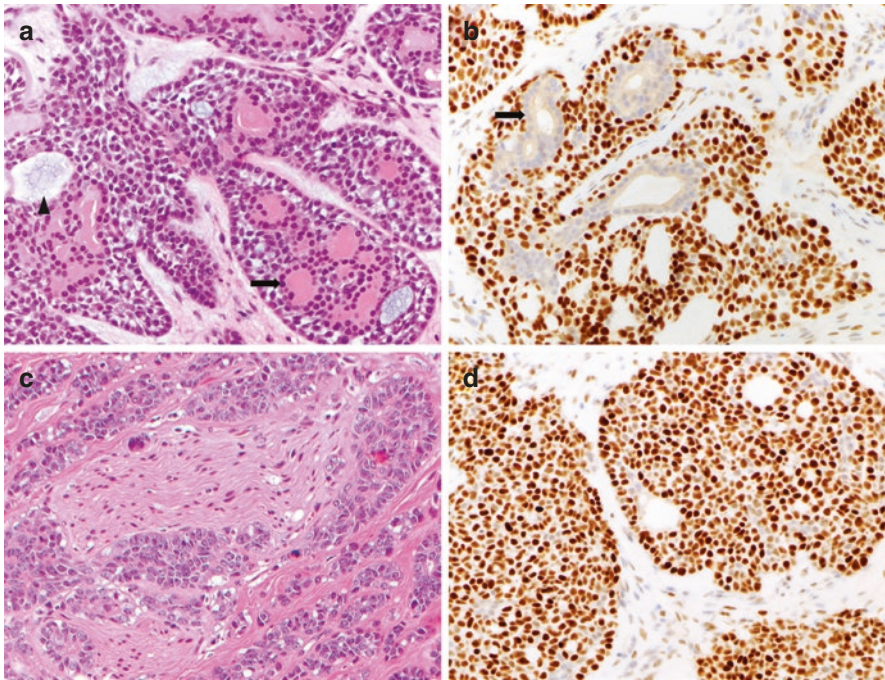


**Fig. 3.5** Adenoid cystic carcinoma. Classical tumors show a cribriform pattern formed by nests of basaloid cells that contain multiple punched-out spaces (a). The spaces are either lined by ductal-type cells with eosinophilic cytoplasm and well-delineated luminal borders (black arrow), or are filled with basophilic hyaline material produced by the surrounding myoepithelial-type tumor cells (black arrowhead). Immunohistochemical stain for p63 highlights the myoepithelial component but is negative in the ductal component (black arrow) (b). Perineural invasion is often prominent (c). Both the ductal and myoepithelial components in an *MYB*-rearranged case show nuclear over-expression of *MYB* by immunohistochemistry (d)

produced by the myoepithelial-type tumor cells. The tubular pattern is composed of bilayered tubules formed by ductal-type luminal cells surrounded by a basal layer of myoepithelial-type cells. In tumors of higher histologic grade, a solid component is typically evident and comprises sheets of basaloid epithelial cells without apparent lumen formation.

Perineural invasion is prominent in most cases. High-grade transformation into an undifferentiated carcinoma may rarely occur.

By immunohistochemistry, the ductal and myoepithelial components can be distinguished by the expression of CD117 in the former and myoepithelial markers (s100, calponin, CK5/6, smooth muscle actin, p63) in the latter. Both components show nuclear staining for MYB in around 80% of cases with the t(6;9) *MYB-NFIB* translocation and 33% of translocation-negative cases [21]. Approximately 63% of sinonasal adenoid cystic carcinomas harbor the *MYB-NFIB* translocation [21].

One particularly challenging differential diagnostic distinction is between adenoid cystic carcinoma and a more recently described entity, the HPV-related multiphenotypic sinonasal carcinoma (HPV-MS). Similar to adenoid cystic carcinoma, HPV-MS are characterized by morphologic and immunophenotypic evidence of myoepithelial and ductal differentiation, often forming cribriform- and tubular-patterned areas. However, features that are unique to HPV-MS include mucosal epithelial surface dysplasia, an overtly squamous component, and the presence of high-risk HPV, most frequently HPV type 33, which can be detected by PCR or chromogenic in situ hybridization.

## ***Treatment and Prognosis***

Adenoid cystic carcinoma is generally treated with a trimodality approach. Overall survival is currently noted as 91%, 83%, and 61% at 3, 2, and 5 years post diagnosis, respectively [19]. Clinicopathologic features reportedly predictive of unfavorable survival include location in the frontal sinus or mixed sites primary, positive margin, perineural or lymphovascular invasion, urban residency, high histologic grade, and advanced stage [19, 21].

## **Mucosal Melanoma**

### ***Definition and Clinical Background***

Mucosal melanomas arise from the intramucosal melanocytes that are normally present but often inconspicuous in the basal aspect of respiratory epithelium and in the submucosal seromucinous glands. The highest incidence is seen in the seventh decade of life with equal gender distribution. Most cases present as a polypoid mass in the nasal cavity or septum.

## Pathology

Mucosal melanomas are characterized by diffuse sheets of epithelioid neoplastic cells with prominent nucleoli, variable amount of eosinophilic cytoplasm, and brisk mitotic activity (Fig. 3.6). Less commonly, the tumor cells may appear spindled or plasmacytoid. The amount of melanin production is variable, with about half of the cases being amelanotic. Immunophenotypically, the tumor cells are positive for S100, HMB-45, melan A, tyrosinase, SOX10, and MITF. Staining intensity of each marker may vary between individual cases, and therefore concurrent use of two to three melanocytic markers may increase the overall sensitivity.

The genetic landscape of mucosal melanomas differs from that of cutaneous and ocular melanomas. The most frequent mutations are in the *NRAS* (19%) and *KIT* (8%) genes [22]. *BRAF* V600E mutations, while detected in the majority of cutaneous melanomas, are present in only 3% of mucosal melanoma [22]. Mutations that are common in ocular melanomas, such as *BAP1*, *GNAQ*, and *GNA11* mutations, are rare in mucosal melanomas.

## Treatment and Prognosis

Mucosal melanomas are treated with surgery and radiotherapy. Metastatic and unresectable cases may receive immunotherapy with checkpoint inhibitors. Cases with *KIT* alterations may consider imatinib therapy although resistance is common [23]. The 3-, 5-, and 15-year overall survival rates of primary sinonasal mucosal melanomas were 50%, 33%, and 14.3%, respectively, in a recent study [24]. In the current (eighth) edition of the American Joint Committee on Cancer (AJCC) staging system, all sinonasal mucosal melanomas are staged as T3 or T4 disease. Nasal cavity origin and lower disease stage (T3) have been associated with better survival [24].

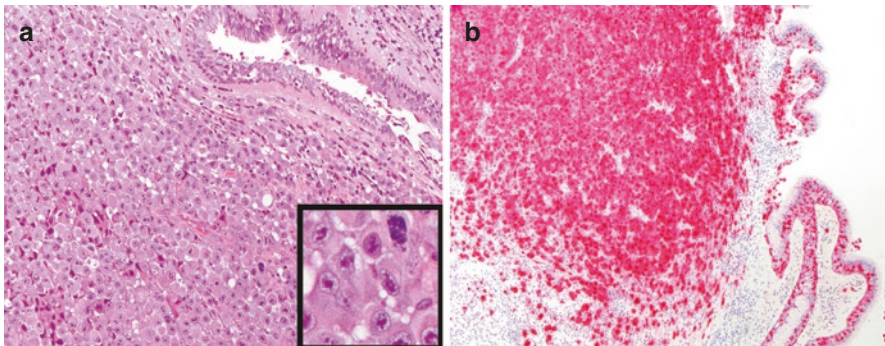


**Fig. 3.6** Mucosal melanoma, composed of diffuse growth of epithelioid tumor cells with prominent nucleoli (a, inset). A melan-A immunostain highlights the expansile tumor as well as adjacent melanoma in situ (b)

## Olfactory Neuroblastoma

### *Definition and Clinical Background*

Olfactory neuroblastoma (ONB), also known as esthesioneuroblastoma, arises from the bipolar neurons in the specialized olfactory epithelium that lines the superior portion of the nasal cavity near the cribriform plate. Patients present across a wide age range from toddlers to the ninth decade of life, with an average age of 53 years and a slight male predilection (male-to-female ratio around 1.4). At initial presentation, 19%, 29%, 18%, and 34% of patients were at Kadish stage A, B, C, and D, respectively [25].

### *Pathology*

Olfactory neuroblastomas can be graded using the Hyams system into grades I, II, III, and IV based on the architecture, mitotic activity, nuclear pleomorphism, fibrillary matrix, rosette formation, and necrosis [1]. At low magnification, low-grade tumors appear as well-demarcated submucosal tumor nests separated by edematous hypocellular stroma (Fig. 3.7). At higher magnification, tumor nests are composed of uniform neoplastic cells with small round nuclei, stippled chromatin, and scant granular cytoplasm, in a compact arrangement or occasionally forming pseudorosettes that surround a central core of neuropil (Homer-Wright pseudorosettes).

With increasing histologic grade, tumors lose the nested architecture and gradually become sheet-forming with loss of neuropil. Concurrently, elevated mitotic activity, necrosis, and nuclear pleomorphism are typically present. Rosettes formed by hyperchromatic tumor cells with true central lumen formation (Flexner-Wintersteiner rosettes) are mostly encountered in Hyams grade III–IV tumors. By immunohistochemistry, the neoplastic cells diffusely express neuroendocrine markers (synaptophysin, chromogranin, CD56, neuron-specific enolase). Besides, NKX2.2 is expressed by 80% of the cases. Sustentacular cells, most easily identified at the periphery of tumor nests in low-grade cases, stain positively for S100. About one-third of cases are focally positive for low-molecular-weight cytokeratins such as Cam5.2 and CK18 [1].

### *Treatment and Prognosis*

Olfactory neuroblastomas are treated with a trimodality approach. According to a SEER analysis of cases between 1973 and 2014, the 5-year overall and cancer-specific survival rates were 69% and 78%, respectively [26]. Better overall and cancer-specific survival rates have been associated with younger age, lower clinical

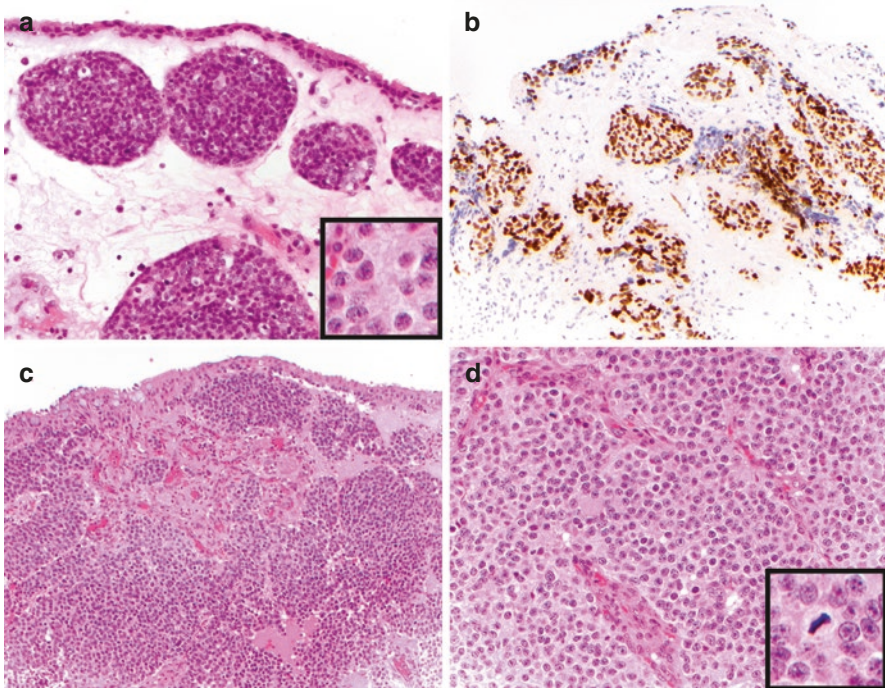


**Fig. 3.7** Olfactory neuroblastoma. A Hyams grade 1 case with well-demarcated submucosal tumor lobules composed of uniform cells with small round nuclei (**a**). The tumor lobules are predominantly solid, with scattered Homer-Wright pseudorosettes that contain central neuropil (**a**, inset). In addition to neuroendocrine markers, most olfactory neuroblastomas also express diffuse NKX2.2 (**b**). A Hyams grade 2 case shows vaguely lobulated diffuse patterns (**c**) with increased mitotic activity (**d**, inset). Cytologic pleomorphism is minimal, and there is abundant fibrillary matrix formation (**d**)

stage, and surgical intervention [26]. High Hyams grade (III–IV) has been found predictive of worse overall survival [27].

## Ewing Sarcoma/Peripheral Primitive Neuroectodermal Tumor

### *Definition and Clinical Background*

The Ewing sarcoma family of tumors (ESFTs) encompasses a group of round cell sarcomas that harbor the pathognomonic *EWSR1* gene rearrangements and show variable neuroectodermal differentiation. The histologic spectrum includes conventional (undifferentiated) Ewing sarcoma and cases with more pronounced neuroectodermal differentiation (peripheral primitive neuroectodermal tumors, pPNET).

Only around 5–10% of ESFTs occur in the head and neck region, including the craniofacial bones (49%), soft tissue and nerves (33%), sinonasal tract (4%), orbit (2%), and parotid gland (2%) [28]. Primary head and neck ESFTs (HN-ESFTs) present at an average age of 25 years with equal gender distribution. Compared to ESFTs arising in other locations, HN-ESFTs tend to present at an earlier stage, with smaller tumor size and more often localized disease at the time of diagnosis [28].

## **Pathology**

Approximately 95% of HN-ESFTs are conventional Ewing sarcomas composed of loose lobules of monotonous round tumor cells with evenly distributed chromatin, small nucleoli, scant pale cytoplasm, and indistinct cell borders. Peripheral primitive neuroectodermal tumors account for the remaining 5% of HN-ESFTs, characterized by neuroectodermal-type rosette formation with central neuropil (Homer-Wright rosette) or true lumens (Flexner-Wintersteiner rosette).

Immunohistochemically, ESFTs show characteristic membranous positivity for CD99 and nuclear expression of FLI1 and NKX2.2. Other immunostains that can be focally positive include some keratins and synaptophysin; the latter, if ordered initially, may be a pitfall suggestive of ONB.

The diagnosis of ESFTs requires molecular confirmation of reciprocal *EWSR1* gene translocations by fluorescence in situ hybridization or reverse transcription polymerase chain reaction. Around 85% of EFSTs are caused by the t(11;22) (q24;q12) translocation, which combines the transcription-regulating domain of *EWSR1* and the DNA-binding domain of *FLI1* into an *EWSR1-FLI1* oncoprotein encoded by fused sequences from the *EWSR1* and *FLI1* genes. *EWSR1-FLI1* acts as an aberrant transcription factor that targets various genes such as NKX2.2, DAX-1, *GLI1*, and the forkhead box (FOX) family of transcription factors [29]. Minor subsets of ESFTs are associated with alternative *EWSR1* translocations such as *EWSR1-ERG*, *EWSR1-ETV1*, *EWSR1-ETV4*, and *EWSR1-FEV*.

The adamantinoma-like Ewing sarcoma (ALES) is a rare but noteworthy variant in the head and neck with increasing recognition. ALES is a tumor of young adults with a propensity for the head and neck region, including the sinonasal tract, parotid gland, and the thyroid [30]. The unusual characteristics of ALES include overt morphologic and immunophenotypic evidence of epithelial differentiation. Most reported cases show a nested growth pattern accompanied by peripheral palisading and focal keratinization of tumor cells (Fig. 3.8a, b). There is diffuse and strong expression of pancytokeratin, p40 (Fig. 3.8c), and synaptophysin (Fig. 3.8d), rendering this entity prone to being interpreted as squamous cell carcinoma (SCC) or neuroendocrine carcinoma (NEC). The diagnostic key is the expression of CD99 (Fig. 3.8e) and NKX2.2 in ALES, absent in SCC and NEC. ALES harbor the *EWSR1-FLI1* translocation, and molecular confirmation is required for rendering the diagnosis [30].

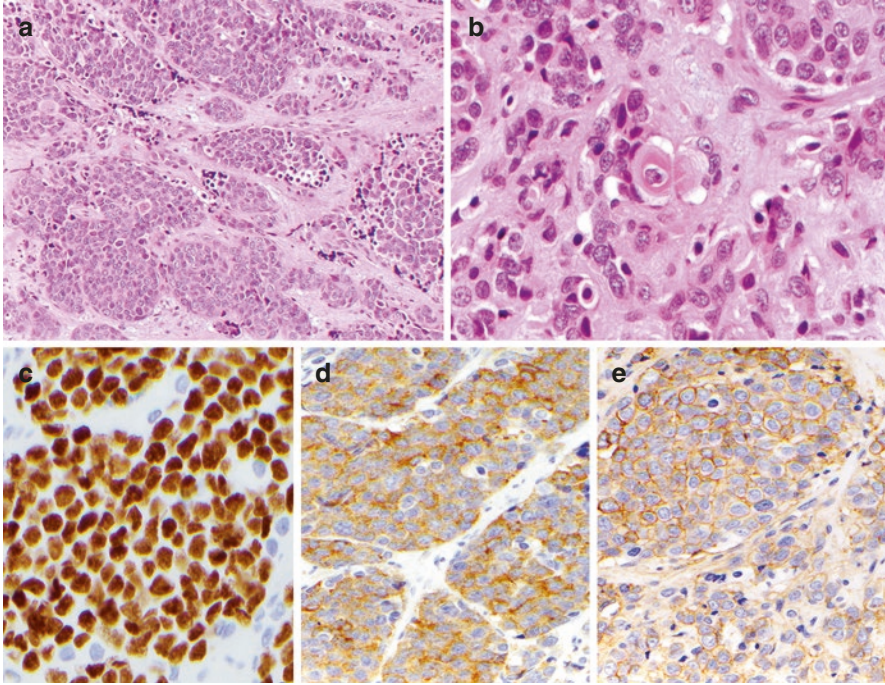


**Fig. 3.8** Adamantinoma-like Ewing sarcoma, with nested growth of monotonous neoplastic cells (a). Focal keratinization is present (b). There is diffuse immunopositivity for p40 (c) and synaptophysin (d), which may lead to an erroneous diagnosis of squamous cell carcinoma or neuroendocrine carcinoma. However, the membranous CD99 staining reveals this lesion being within the Ewing sarcoma family of tumors (e)

### *Treatment and Prognosis*

According to a recent analysis of the SEER database between 1993 and 2013, the 10-year overall survival for primary head and neck Ewing sarcoma was 69%, significantly higher than Ewing sarcoma in other sites (54%) [28]. The study also found older age, Black/Hispanic race, large tumor size, and distant metastatic disease to be associated with worse prognosis [28].

## **Rhabdomyosarcoma**

### *Definition and Clinical Background*

Primary sarcomas account for less than 5% of sinonasal malignancies, with rhabdomyosarcoma (RMS) being the most common histologic type in both children and adults (overall constituting 33% of cases), followed by osteosarcoma (26%), chondrosarcoma (19%), fibrosarcoma (11%), Ewing sarcoma (4%), and leiomyosarcoma

(4%) [31]. Rhabdomyosarcomas typically present as polypoid submucosal masses. The overall incidence is highest in the first decade of life with no gender difference.

### ***Pathology***

The embryonal, alveolar, and spindle cell subtypes of rhabdomyosarcoma all may occur in the sinonasal tract. Among pediatric patients, embryonal rhabdomyosarcoma is the predominant form, characterized by primitive round to short spindled cells with scant cytoplasm in a diffuse growth pattern. Rhabdomyoblasts showing eccentric nuclei and brightly eosinophilic cytoplasm may be present. In the “botryoid” pattern of embryonal rhabdomyosarcoma, there is a subepithelial zone of tumor cell concentration, often referred to as a “cambium layer” (Fig. 3.9a, b). In adult patients, the alveolar subtype is the most common. Alveolar rhabdomyosarcomas harbor the t(2;13) (*PAX3-FOXO1*) or t(1;13) (*PAX7-FOXO1*) translocation, and are histologically characterized by an alveolar growth pattern with delicate fibrous septa separating pockets of round monotonous tumor cells (Fig. 3.9c, d). The rare spindle cell subtype has fascicular growth of spindle cells with elongated nuclei. The diagnostic key is the identification of elevated mitotic activity and interspersed spindled tumor cells with brightly eosinophilic cytoplasm. All the three subtypes are immunohistochemically positive for desmin, myogenin, MYOD1, and muscle-specific actin.

### ***Treatment and Prognosis***

Sinonasal rhabdomyosarcomas are treated with surgery and chemoradiation, with overall poor prognosis. Among the adult population in the United States, the 5-year overall survival was 28.4% per a nationwide study between 2004 and 2013 [32]. Age under 35 years and localized disease are associated with better overall survival [32]. In pediatric patients, the 5-, 10-, and 20-year disease-specific survival rates are 53%, 41%, and 22%, respectively, based on a recent analysis of the SEER database between 1973 and 2013 [33].

## **Extranodal NK-/T-Cell Lymphoma (ENKTL)**

### ***Definition and Clinical Background***

Virtually all primary sinonasal lymphomas are non-Hodgkin lymphomas. The predominant histological subtype varies with geographic regions and anatomic locations. In the United States and Europe, diffuse large B-cell lymphoma is the most common histologic type and the maxillary sinus is the most frequent primary site.

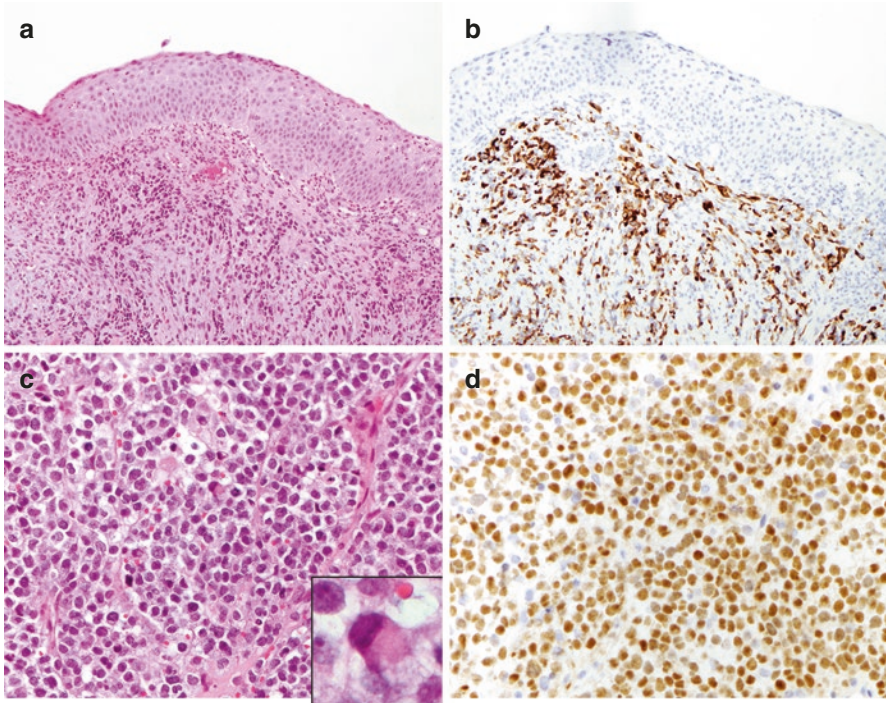


**Fig. 3.9** Rhabdomyosarcoma. (a, b) The embryonal type shows a subepithelial zone of tumor cell condensation (a), more easily identified with desmin immunostain (b). (c, d) This alveolar rhabdomyosarcoma harbors a t(2;13) (q35;q14), PAX3/FOXO1 translocation. Morphologically, the tumor consists of monotonous small round cells with scant clear cytoplasm, divided into vague lobules by delicate fibrous septa (c). Scattered rhabdomyoblasts with eccentric nuclei and brightly eosinophilic cytoplasm are present (c, inset). There is diffuse nuclear expression of MYOD1 (d)

Among East Asians and indigenous populations of the Central and South America, extranodal NK-/T-cell lymphoma (ENKTL) accounts for most sinonasal lymphoma cases with a propensity for the nasal cavity.

Extranodal NK-/T-cell lymphoma (ENKTL), nasal type, is universally associated with the oncogenic Epstein–Barr virus (EBV). The historical term for this aggressive tumor type, “lethal midline granuloma,” succinctly summarizes its clinical features. Most patients present with nasal obstruction and bleeding. Advanced cases may have central facial ecchymosis, ulceration, or orbital involvement.

### **Pathology**

The histologic hallmarks of ENKTL include the following: (1) a diffuse pattern with mixed inflammation, and (2) angiocentric/angioinvasive tumor growth causing extensive necrosis (Fig. 3.10). The neoplastic cells are large with folded, variably

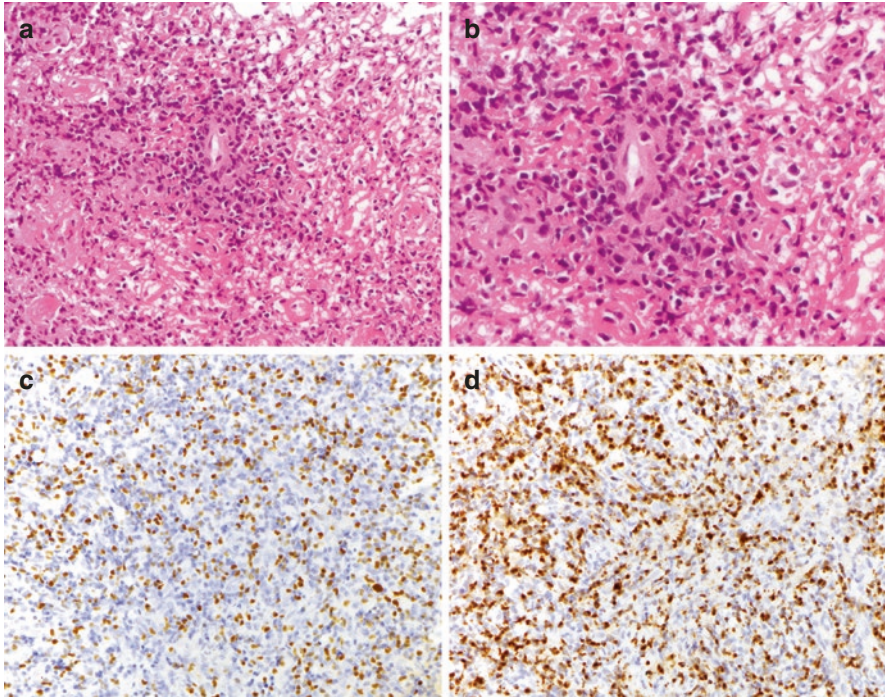


**Fig. 3.10** Extranodal NK-/T-cell lymphoma, nasal type. At low magnification, there are abundant lymphocytic infiltrates in a fibrinous background (a). At high magnification, most lymphocytic cells appear large, with moderate anisonucleosis and irregular nuclear membranes, with angiocentric infiltration into a small vessel (b). The lesional lymphocytes are positive for EBV (c, in situ hybridization) and granzyme B (d, immunohistochemistry)

sized nuclei and small nucleoli. Immunohistochemically, the tumor cells present a cytotoxic phenotype with expression of CD3, CD56, TIA1, granzyme B, and perforin. CD4, CD5, and CD8 are generally negative. A positive result for chromogenic in situ hybridization for EBV is essential for rendering the diagnosis. Cases that have similar pathologic features but lack EBV are considered peripheral T-cell lymphoma, not otherwise specified [1].

ENKTL may be easily misinterpreted, especially in small biopsies, as a reactive or vasculitic process (e.g., granulomatosis with polyangiitis) given the presence of necrosis and mixed inflammatory infiltrates that may obscure the presence of neoplastic cells. A high index of clinical suspicion and a screening EBV in situ hybridization test for suspicious cases are therefore of practical benefit. Lymphoepithelial carcinoma (LEC) is another EBV-positive tumor in the sinonasal tract. The neoplastic cells in LEC are larger, with prominent nucleoli and positive immunostains for pancytokeratin, cytokeratin 5/6, and p40.

## ***Treatment and Prognosis***

Patients with ENKTL are generally treated with radiotherapy (RT) and chemotherapy (CT). A recent meta-analysis suggested a survival benefit in upfront combined RT and CT, as compared to a sequential approach with induction CT followed by RT [34]. Other favorable prognostic factors include low clinical stage (Ann Arbor stage I/II) and younger age (under 60 years). In a recent study where 76% of patients presented at Ann Arbor stage I/II, the 5-year progression-free and overall survival rates were 49.9% and 54.8%, respectively [35].

## **Sinonasal Undifferentiated Carcinoma (SNUC)**

### ***Definition and Clinical Background***

SNUC is currently a diagnosis of exclusion, with an expanding list of morphologic mimics to be considered before rendering the diagnosis. It was first described in 1986 by Frierson et al. in a series of locally advanced, highly fatal sinonasal tumors composed of nests, trabeculae, and sheets of medium-sized neoplastic cells with epithelial differentiation (cytokeratin positivity) and high-grade cytologic features [36]. The incidence is around 0.2 cases per million population, accounting for 3–5% of sinonasal carcinomas. Patient age ranges widely from the second to the eighth decade of life, with an approximately 2:1 male-to-female ratio [37]. Around 80% of the cases in the United States are in Caucasians. The nasal cavity and the ethmoid sinus are the most frequently affected locations. At initial presentation, over 80% are T4 disease and around 16% have lymph node metastases [38].

### ***Pathology***

Histologically, SNUCs are composed of nests, trabeculae, and sheets of somewhat monotonous cells with hyperchromatic to vesicular nuclei and often prominent nucleoli (Fig. 3.11). There is by definition no squamous or glandular differentiation. Mitotic activity and necrosis are often abundant. By immunohistochemistry, the tumor cells are positive for pancytokeratin and CK7 but are negative for squamous cell markers such as CK5/6 and p40. Expression of neuroendocrine markers (synaptophysin and chromogranin) may be focally present but should not be as strong and diffuse as in neuroendocrine carcinomas. In situ hybridization for both HPV and EBV is usually negative.

Most recently, recurrent mutations of the catalytic site residue R172 of the isocitrate dehydrogenase 2 (IDH2) are found in over 80% of SNUCs and 50% of large cell neuroendocrine carcinoma (LCNEC), suggesting that SNUCs and LCNEC may form a spectrum of genetically similar disease [39]. *IDH2* R172 mutations also

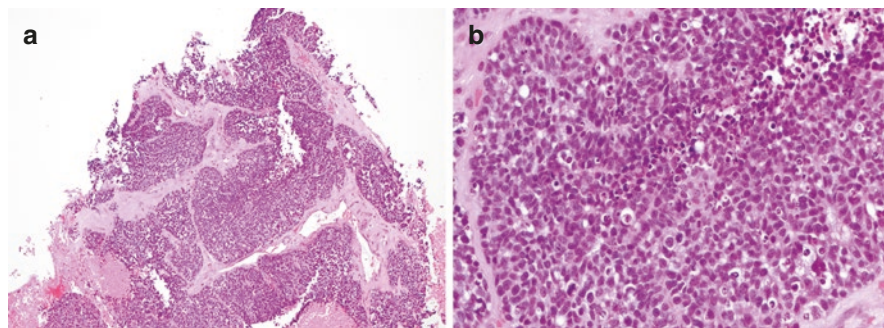


**Fig. 3.11** Sinonasal undifferentiated carcinoma. This infiltrative tumor consists entirely of sheets of round cells with brisk mitotic activity and lacks squamous or glandular differentiation ((a), low magnification; (b), high magnification). Immunophenotypically, there is diffuse expression of AE1/AE3, Cam5.2, and CK7. The tumor cells are otherwise negative for neuroendocrine and melanocytic markers as well as desmin, CD45, CD99, EBER, and high-risk HPV. INI1 and BRG1 are retained, and a NUT stain is negative (see Chap. 12 for details about these three stains)

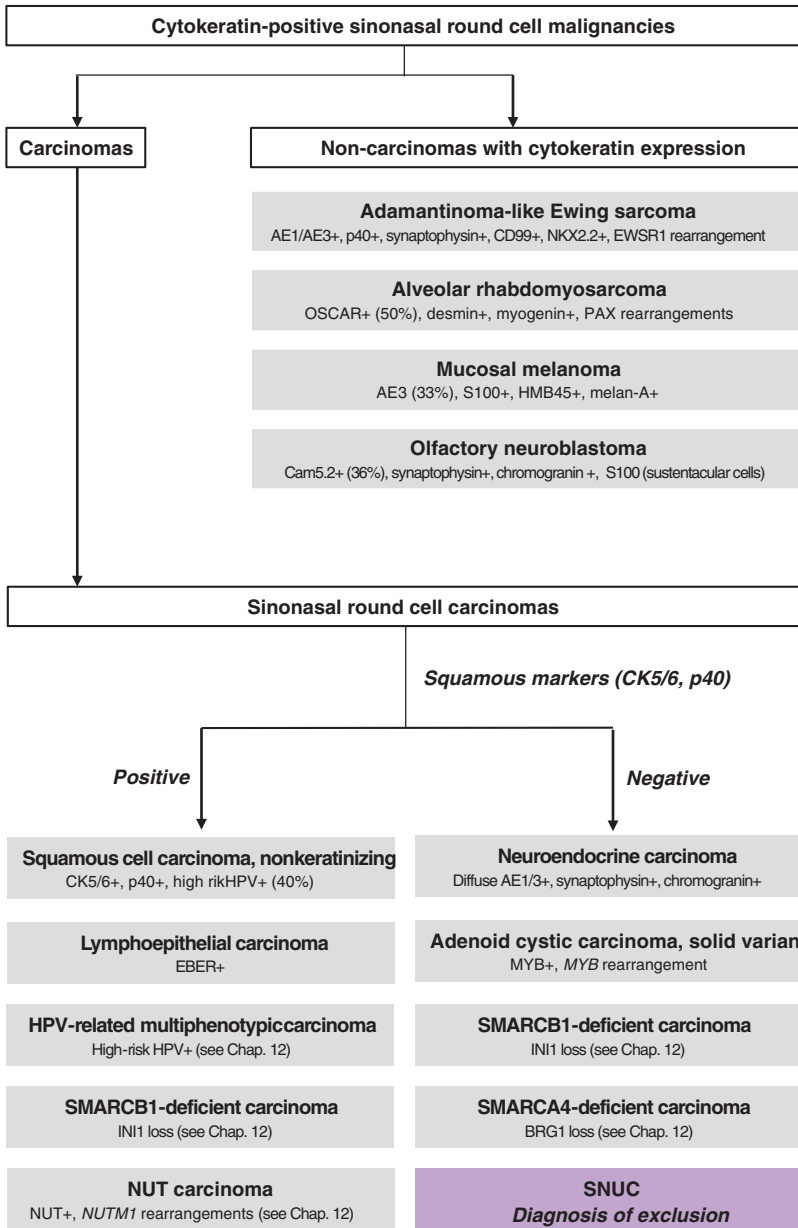
occur in the angioimmunoblastic lymphoma, acute myeloid leukemia, oligodendroglioma, astrocytoma, intrahepatic cholangiocarcinoma, and chondrosarcoma. The mutant IDH enzyme loses its physiologic function in converting isocitrate to alpha-ketoglutarate ( $\alpha$ -KG); instead, it gains a new catalytic ability in converting  $\alpha$ -KG to an oncometabolite 2-hydroxyglutarate (2-HG). Intracellular accumulation of 2-HG, a structurally similar antagonist to  $\alpha$ -KG, leads to the inhibition of several  $\alpha$ -KG-dependent epigenetic modification enzymes, including DNA demethylases and histone lysine demethylases, as well as the alkB homolog (ALKBH) DNA repair enzymes. Thus, *IDH2* mutated tumors characteristically show a global hypermethylator phenotype, which was recently demonstrated in SNUCs [40]. The hypermethylated genomic status is believed to block cell differentiation and leads to the undifferentiated morphology of these tumors.

The differential diagnosis for SNUC is broad. Several non-epithelial tumors may have focal to diffuse cytokeratin expression, including alveolar rhabdomyosarcoma (50% positive for pancytokeratin OSCAR, 52% for Cam5.2), mucosal melanoma (33% for AE3, 25% for CK7, 22% for EMA), and olfactory neuroblastoma (43% for CK18, 36% for Cam5.2).

Adamantinoma-like Ewing sarcoma, as discussed earlier, is a rare *EWSR1*-rearranged tumor characterized by monotonous undifferentiated cytology and diffuse immunoreactivity for AE1/AE3, p40, synaptophysin, and the Ewing sarcoma markers (CD99, NKX2.2). Recently, several groups of high-grade sinonasal carcinomas that used to be within the SNUC category have now been re-classified as independent molecularly defined entities. These include NUT carcinoma (defined by *NUTM1* gene rearrangements), the SMARCB1-deficient sinonasal carcinoma (defined by the loss of SMARCB1/INI1 expression mostly due to *SMARCB1* gene deletions), and the SMARCA4-deficient sinonasal carcinoma (defined by the loss of SMARCA4/BRG1 expression mostly due to *SMARCA4* gene deleterious mutations). In addition, high-grade HPV- and EBV-related carcinomas, solid variant of

adenoid cystic carcinoma, and neuroendocrine carcinoma are also in the differential list for high-grade sinonasal tumors. A summary of the differential diagnostic procedure for cytokeratin-positive poorly differentiated sinonasal malignancies with round cell morphology is outlined in Algorithm 3.1.

**Algorithm 3.1**



## ***Treatment and Prognosis***

SNUCs are aggressive tumors with high mortality. Median survival of all patients was 22.1 months according to a recent analysis of nationwide data in the United States [37]. Overall survival rates were 44.3%, 34.9%, and 31.3% at 3, 5, and 10 years post diagnosis, respectively. Radiation and combined surgery and radiation were each associated with improved survival [37]. The recent discovery of *IDH2* hotspot mutations raises the possibility of targeted therapy.

Enasidenib is a mutant *IDH2* inhibitor currently approved by the United States Food and Drug Administration for the treatment of acute myeloid leukemia harboring *IDH2* R172 mutations. Several phase 1 and 2 clinical trials are ongoing in gliomas and other solid tumors (<https://www.clinicaltrials.gov/>).

## **References**

1. El-Naggar AK, Grandis JR, Takata T, Slootweg PJ, editors. WHO classification of head and neck tumours. Lyon: International Agency for Research on Cancer; 2017.
2. Grau C, et al. Sino-nasal cancer in Denmark 1982-1991--a nationwide survey (in eng). *Acta Oncol*. 2001;40(1):19–23. <https://doi.org/10.1080/028418601750070993>.
3. Gore MR. Survival in sinonasal and middle ear malignancies: a population-based study using the SEER 1973–2015 database (in eng). *BMC Ear Nose Throat Disord*. 2018;18:13. <https://doi.org/10.1186/s12901-018-0061-4>.
4. Kilic S, Samarrai R, Kilic SS, Mikhael M, Baredes S, Eloy JA. Incidence and survival of sinonasal adenocarcinoma by site and histologic subtype (in eng). *Acta Otolaryngol*. 2018;138(4):415–21. <https://doi.org/10.1080/00016489.2017.1401229>.
5. Llorente JL, Lopez F, Suarez C, Hermsen MA. Sinonasal carcinoma: clinical, pathological, genetic and therapeutic advances (in eng). *Nat Rev Clin Oncol*. 2014;11(8):460–72. <https://doi.org/10.1038/nrclinonc.2014.97>.
6. Lewis JS Jr. Sinonasal squamous cell carcinoma: a review with emphasis on emerging histologic subtypes and the role of human papillomavirus (in eng). *Head Neck Pathol*. 2016;10(1):60–7. <https://doi.org/10.1007/s12105-016-0692-y>.
7. Ansa B, et al. Paranasal sinus squamous cell carcinoma incidence and survival based on Surveillance, Epidemiology, and End Results data, 1973 to 2009 (in eng). *Cancer*. 2013;119(14):2602–10. <https://doi.org/10.1002/cncr.28108>.
8. Bishop JA, et al. Human papillomavirus-related carcinomas of the sinonasal tract (in eng). *Am J Surg Pathol*. 2013;37(2):185–92. <https://doi.org/10.1097/PAS.0b013e3182698673>.
9. Jiomaru R, et al. HPV-related sinonasal carcinoma: clinicopathologic features, diagnostic utility of p16 and Rb immunohistochemistry, and EGFR copy number alteration (in eng). *Am J Surg Pathol*. 2020;44(3):305–15. <https://doi.org/10.1097/pas.0000000000001410>.
10. Chen MM, Roman SA, Sosa JA, Judson BL. Predictors of survival in sinonasal adenocarcinoma (in eng). *J Neurol Surg B Skull Base*. 2015;76(3):208–13. <https://doi.org/10.1055/s-0034-1543995>.
11. Donhuijsen K, Kollerker I, Petersen P, Gassler N, Wolf J, Schroeder HG. Clinical and morphological aspects of adenocarcinomas of the intestinal type in the inner nose: a retrospective multicenter analysis (in eng). *Eur Arch Otorhinolaryngol*. 2016;273(10):3207–13. <https://doi.org/10.1007/s00405-016-3987-4>.
12. Barnes L. Intestinal-type adenocarcinoma of the nasal cavity and paranasal sinuses (in eng). *Am J Surg Pathol*. 1986;10(3):192–202. <https://doi.org/10.1097/0000478-198603000-00006>.

13. Tilson MP, Gallia GL, Bishop JA. Among sinonasal tumors, CDX-2 immunexpression is not restricted to intestinal-type adenocarcinomas (in eng). *Head Neck Pathol.* 2014;8(1):59–65. <https://doi.org/10.1007/s12105-013-0475-7>.
14. Holmila R, et al. Mutations in TP53 tumor suppressor gene in wood dust-related sinonasal cancer (in eng). *Int J Cancer.* 2010;127(3):578–88. <https://doi.org/10.1002/ijc.25064>.
15. Andreasen S, et al. ETV6 gene rearrangements characterize a morphologically distinct subset of sinonasal low-grade non-intestinal-type adenocarcinoma: a novel translocation-associated carcinoma restricted to the sinonasal tract (in eng). *Am J Surg Pathol.* 2017;41(11):1552–60. <https://doi.org/10.1097/pas.0000000000000912>.
16. Antognoni P, et al. Endoscopic resection followed by adjuvant radiotherapy for sinonasal intestinal-type adenocarcinoma: retrospective analysis of 30 consecutive patients (in eng). *Head Neck.* 2015;37(5):677–84. <https://doi.org/10.1002/hed.23660>.
17. Bignami M, et al. Sinonasal non-intestinal-type adenocarcinoma: a retrospective review of 22 patients (in eng). *World Neurosurg.* 2018;120:e962–9. <https://doi.org/10.1016/j.wneu.2018.08.201>.
18. Hay AJ, Migliacci J, Karassawa Zanoni D, McGill M, Patel S, Ganly I. Minor salivary gland tumors of the head and neck-Memorial Sloan Kettering experience: incidence and outcomes by site and histological type (in eng). *Cancer.* 2019;125(19):3354–66. <https://doi.org/10.1002/cncr.32208>.
19. Trope M, et al. Adenoid cystic carcinoma of the sinonasal tract: a review of the national cancer database (in eng). *Int Forum Allergy Rhinol.* 2019;9(4):427–34. <https://doi.org/10.1002/alr.22255>.
20. Rhee CS, et al. Adenoid cystic carcinoma of the sinonasal tract: treatment results (in eng). *Laryngoscope.* 2006;116(6):982–6. <https://doi.org/10.1097/01.mlg.0000216900.03188.48>.
21. Thompson LD, et al. Sinonasal tract and nasopharyngeal adenoid cystic carcinoma: a clinicopathologic and immunophenotypic study of 86 cases (in eng). *Head Neck Pathol.* 2014;8(1):88–109. <https://doi.org/10.1007/s12105-013-0487-3>.
22. Zebary A, Jangard M, Omholt K, Ragnarsson-Olding B, Hansson J. KIT, NRAS and BRAF mutations in sinonasal mucosal melanoma: a study of 56 cases (in eng). *Br J Cancer.* 2013;109(3):559–64. <https://doi.org/10.1038/bjc.2013.373>.
23. Hodi FS, et al. Imatinib for melanomas harboring mutationally activated or amplified KIT arising on mucosal, acral, and chronically sun-damaged skin (in eng). *J Clin Oncol.* 2013;31(26):3182–90. <https://doi.org/10.1200/jco.2012.47.7836>.
24. Dreno M, et al. Sinonasal mucosal melanoma: a 44-case study and literature analysis (in eng). *Eur Ann Otorhinolaryngol Head Neck Dis.* 2017;134(4):237–42. <https://doi.org/10.1016/j.anorl.2017.02.003>.
25. Cranmer LD, Chau B, Rockhill JK, Ferreira M Jr, Liao JJ. Chemotherapy in esthesioneuroblastoma/olfactory neuroblastoma: an analysis of the surveillance epidemiology and end results (SEER) 1973-2015 database (in eng). *Am J Clin Oncol.* 2020;43(3):203–9. <https://doi.org/10.1097/coc.0000000000000649>.
26. Yin Z, et al. Age distribution and age-related outcomes of olfactory neuroblastoma: a population-based analysis (in eng). *Cancer Manag Res.* 2018;10:1359–64. <https://doi.org/10.2147/cmar.s151945>.
27. Van Gompel JJ, et al. Long-term outcome of esthesioneuroblastoma: hyams grade predicts patient survival (in eng). *J Neurol Surg B Skull Base.* 2012;73(5):331–6. <https://doi.org/10.1055/s-0032-1321512>.
28. Ellis MA, Gerry DR, Neskey DM, Lentsch EJ. Ewing sarcoma of the head and neck (in eng). *Ann Otol Rhinol Laryngol.* 2017;126(3):179–84. <https://doi.org/10.1177/0003489416681322>.
29. Cidre-Aranaz F, Alonso J. EWS/FLI1 target genes and therapeutic opportunities in Ewing sarcoma (in eng). *Front Oncol.* 2015;5:162. <https://doi.org/10.3389/fonc.2015.00162>.
30. Bishop JA, Alaggio R, Zhang L, Seethala RR, Antonescu CR. Adamantinoma-like Ewing family tumors of the head and neck: a pitfall in the differential diagnosis of basaloid and

- myoepithelial carcinomas (in eng). *Am J Surg Pathol*. 2015;39(9):1267–74. <https://doi.org/10.1097/pas.0000000000000460>.
31. Kauke M, Safi AF, Grandoch A, Nickenig HJ, Zoller J, Kreppel M. Sarcomas of the sinonasal tract (in eng). *Head Neck*. 2018;40(6):1279–86. <https://doi.org/10.1002/hed.25108>.
  32. Stepan K, et al. Outcomes in adult sinonasal rhabdomyosarcoma (in eng). *Otolaryngol Head Neck Surg*. 2017;157(1):135–41. <https://doi.org/10.1177/0194599817696287>.
  33. Chung SY, Unsal AA, Kilic S, Baredes S, Liu JK, Eloy JA. Pediatric sinonasal malignancies: a population-based analysis (in eng). *Int J Pediatr Otorhinolaryngol*. 2017;98:97–102. <https://doi.org/10.1016/j.ijporl.2017.04.032>.
  34. Hu S, Zhou D, Zhang W. The optimal timing of radiotherapy in the combined modality therapy for limited-stage extranodal NK/T cell lymphoma (ENKTL): a systematic review and meta-analysis (in eng). *Ann Hematol*. 2018;97(12):2279–87. <https://doi.org/10.1007/s00277-018-3479-2>.
  35. Su YJ, et al. Extranodal NK/T-cell lymphoma, nasal type: clinical features, outcome, and prognostic factors in 101 cases (in eng). *Eur J Haematol*. 2018;101(3):379–88. <https://doi.org/10.1111/ejh.13126>.
  36. Frierson HF, Mills SE, Fechner RE, Taxy JB, Levine PA. Sinonasal undifferentiated carcinoma. An aggressive neoplasm derived from schneiderian epithelium and distinct from olfactory neuroblastoma (in eng). *Am J Surg Pathol*. 1986;10(11):771–9.
  37. Chambers KJ, et al. Incidence and survival patterns of sinonasal undifferentiated carcinoma in the United States (in eng). *J Neurol Surg B Skull Base*. 2015;76(2):94–100. <https://doi.org/10.1055/s-0034-1390016>.
  38. Lin EM, et al. Sinonasal undifferentiated carcinoma: a 13-year experience at a single institution (in eng). *Skull Base*. 2010;20(2):61–7. <https://doi.org/10.1055/s-0029-1236165>.
  39. Dogan S, et al. Frequent IDH2 R172 mutations in undifferentiated and poorly-differentiated sinonasal carcinomas (in eng). *J Pathol*. 2017;242(4):400–8. <https://doi.org/10.1002/path.4915>.
  40. Dogan S, et al. DNA methylation-based classification of sinonasal undifferentiated carcinoma (in eng). *Mod Pathol*. 2019;32(10):1447–59. <https://doi.org/10.1038/s41379-019-0285-x>.